ISSN 1516-392X

EFFECTS OF CRACK RELATIVE DEPTH ON THE EXPERIMENTAL EVALUATION OF FRACTURE TOUGHNESS OF ASTM A516 GR 70 STEEL ON THE DUCTILE-TO-BRITTLE TRANSITION TEMPERATURE USING SE(B) SPECIMENS[1]

Gustavo Henrique Bolognesi Donato[2]
Sullivan de Souza Dantas[3]

Abstract

Fracture testing of structural steels is usually based on standardized specimens (e.g.: C(T), SE(B)). Current standards usually recommend deep cracks ($a/W \geq 0.45$) to guarantee high levels of stress triaxiality and therefore critical J and CTOD values in the case of Elastic Plastic Fracture Mechanics (EPFM). This approach relies upon the notion that similitude concept is valid since plasticity is limited and SSY conditions are respected. However, pressure vessels and pipelines present membrane stresses combined to shallow cracks and develop low stress triaxiality favoring plasticity. In these cases toughness data from deep cracked specimens can potentially underestimate the load-carrying capacity of real structures (being conservative). As an alternative, shallow cracked specimens can reproduce low triaxiality structures and in some cases more accurately predict failure. The problem is that these geometries develop significant plasticity ahead of the crack tip and fracture toughness results can become geometry-dependent, demanding bi-parametric methodologies (e.g.: J-Q, J-T). Results from the literature regarding fracture toughness of ferritic structural steels on the ductile-to-brittle transition temperature as a function of crack depth are relatively scarce and when available present very large scatter. To better quantify toughness of a ASTM A516 Gr70 steel under different triaxiality levels, this work investigates the effects of shallow ($a/W \approx$ 0.20) and deep cracks ($a/W \approx$ 0.50) on fracture toughness using SE(B) specimens. Approximately 20 specimens (18 mm thick) were tested for each condition at ~ -75ºC and results were evaluated using J-Q theory and Weibull statistics. FE models provided Q values and therefore triaxiality levels. All fracture results could be very well described using two-parameters Weibull distributions. Shallow cracks slightly overestimated toughness (~ 8%), presented larger scatter and provided more non-critical data. In addition, ~ 90% of the fracture toughness data obtained from shallow-cracked samples violated the deformation limits of EPFM (validity of J integral as a single parameter to describe crack-tip stress fields), demanding bi-parametric approaches.

Keywords: Crack depth; Shallow cracks; SE(B) specimens; Fracture toughness; ASTM A516 Gr70 steel.

[1] *Technical contribution to 68th ABM International Congress, July, 30th to August 2nd, 2012, Belo Horizonte, MG, Brazil.*

[2] *Mechanical Engineer. D.Sc., Professor, Mechanical Engineering Dept., FEI University. São Bernardo do Campo, SP, Brazil. gdonato@fei.edu.br*

[3] *Mechanical Engineer. Master student, Mechanical Engineering Dept., FEI University. . São Bernardo do Campo, SP, Brazil. sullivan_fei@hotmail.com*

ISSN 1516-392X

1 INTRODUCTION

Current recommended practices for design and integrity assessment of structural components containing crack-like defects are based on fracture mechanics theory and rely upon the notion that a single parameter which defines the crack driving force characterizes the fracture resistance of the material.[1] If elastic stress-strain fields prevail ahead of the crack tip, these parameters derive from the theoretical background of Linear Elastic Fracture Mechanics (LEFM), where K parameter (also known as the stress intensity factor) is the most useful quantity to characterize the severity of the crack. Conversely, if plastic effects are not negligible, Elastic-Plastic Fracture Mechanics (EPFM) must be employed, whose main quantities are the J-integral and the (analogous) Crack-Tip-Opening Displacement (CTOD, δ). Several recommended methodologies for structural integrity evaluation can be found, for example, in API RP 579,[2] BS 7910,[3] R6,[4] SINTAP[5] or DNV-OS-F101[6] and will not be detailed here due to space limitations. However, in all cases these evaluations must be supported by accurate mechanical properties (experimental fracture toughness results) to provide safe and precise predictions. This is the central motivation for this investigation.

In the case of fracture phenomena experienced by current high-toughness structural steels (for example applicable to pipelines, pressure vessels and other pressurized components), assessments usually demand EPFM parameters. This is the case of this work and, therefore, the crack-driving forces (and the elastic-plastic macroscopic loading) will be characterized here by J-integral and $CTOD$ (δ).

Current most complete and relevant standardized procedures for experimental fracture toughness evaluation are ASTM E1820[7], ASTM E1290[8] and ISO 12135.[9] Those three standards represent unified methods for determining fracture toughness in terms of K, δ and J for homogeneous metallic materials subjected to quasistatic loading. In these standards, Compact under Tension - C(T) and Single-Edge notched under Bending - SE(B) specimens are recommended and employed in most cases. Figure 1 presents the main geometrical features of SE(B) specimens, selected by the authors for this investigation. The main problem is that these standards usually recommend deep-cracked samples ($a/W \geq 0.45$) to guarantee high levels of stress triaxiality and therefore critical J and $CTOD$ values.[1,7-9] This approach tries to guarantee that similitude concept is valid since in deep-cracked geometries plasticity is limited and Small Scale Yielding (SSY) conditions are easily respected.

However, pressure vessels or pipelines present membrane stresses combined to shallow cracks and develop low stress triaxiality favoring plasticity, as can be found on previous work from Moreira and Donato[10] and Cravero and Ruggieri[11] In these cases toughness data from deep cracked specimens can potentially underestimate the load-carrying capacity of real structures (being conservative).[12] As an alternative, shallow cracked specimens can reproduce low triaxiality structures and in some cases more accurately predict failure. The problem is that these geometries develop significant plasticity ahead of the crack tip and experimental fracture toughness results become geometry-dependent, violating SSY conditions and demanding bi-parametric methodologies (e.g.: J-Q, J-T). Results from the literature regarding fracture toughness of ferritic structural steels on the ductile-to-brittle transition temperature as a function of crack depth are relatively scarce and when available present very large scatter. To better quantify toughness of a ASTM A516 Gr70 steel under different triaxiality levels, this work investigates the effects of shallow ($a/W \approx 0.20$) and deep cracks ($a/W \approx 0.50$) on fracture toughness using SE(B)

ISSN 1516-392X

specimens. The main results include: i) fracture toughness data in terms of J and δ described using Weibull statistics; ii) the increase in toughness values due to the use of shallow cracked samples; iii) the corresponding triaxiality levels (in terms of Q) associated to the obtained results; iv) and to which extent shallow cracked SE(B) specimens can provide geometry-independent fracture toughness data to be employed with single parameter fracture mechanics under SSY conditions.

2 *J*-INTEGRAL AND CTOD EXPERIMENTAL ASSESSMENT

Fracture testing of such SE(B) specimens provides load-displacement curves as the one illustrated by Figure 2(a). During the test, the loading is monotonically increased until final fracture takes place. Elastic and plastic areas (respectively A_{el} and A_{pl}) at this moment can be easily computed and allow J and δ estimation using, for example, the eta (η) method as presented by Eqs. (1,2) and recommended by the aforementioned standards.[7-9] In these formulae, K_I denotes the applied stress intensity factor (Eq. 3), $E' = E$ for plane stress conditions or $E' = E/(1-\nu^2)$ for plane strain conditions, m represents a plastic constrain factor,[1] σ_{flow} is defined as the average of yield and ultimate tensile stresses in the form $\sigma_{flow}=(\sigma_{ys}+\sigma_{uts})/2$ and η_J or η_δ factors are nondimensional parameters which describes the effect of plastic strain energy on J and $CTOD$. These factors can be found in Donato, Magnabosco and Ruggieri[13] for SE(B) specimens of varying crack depths. In Eq. (3), $f(a/W)$ represents a nondimensional stress intensity factor and can be found in ASTM E1820 for SE(B) specimens.[7]

$$J = J_{el} + J_{pl} = \frac{K_I^2}{E'} + \frac{\eta_J \cdot A_{pl}}{B \cdot (W-a)} \tag{1}$$

$$\delta = \delta_{el} + \delta_{pl} = \frac{K_I^2}{m \cdot \sigma_{flow} \cdot E'} + \frac{\eta_\delta \cdot A_{pl}}{B \cdot \sigma_{flow} \cdot (W-a)} \tag{2}$$

$$K_I = \frac{P}{B \cdot \sqrt{W}} \cdot f(a/W) \tag{3}$$

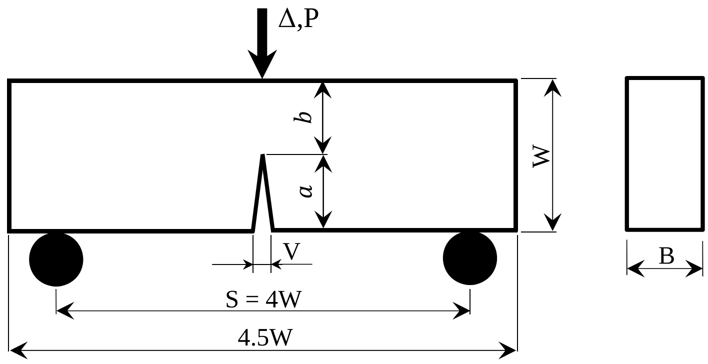

Figure 1. Single edge notched under bending – SE(B) – fracture specimens. P denotes applied load, Δ the Load-Line Displacement (LLD) and V the Crack Mouth Opening Displacement ($CMOD$).

ISSN 1516-392X

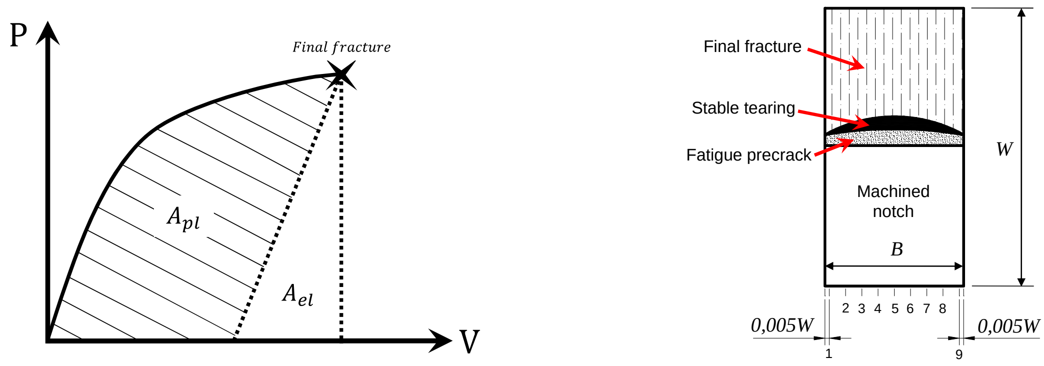

(a) (b)

Figure 2. (a) Schematic load-displacement curve until final fracture in terms of *CMOD* (*V*). (b) Schematic post-mortem examination of an SE(B) specimen.

If the material experiences unstable fracture during testing (e.g.: cleavage in ferritic steels), fracture toughness can be described in terms of critical parameters (denoted J_c or δ_c).[1] However, an additional requirement is necessary to consider fracture toughness as “critical”. As presented by Figure 2(b), stable tearing can take place prior to final fracture, and it must be quantified as the average value of the nine equally spaced measurements parallel to W. If average stable tearing is greater than 0.2 mm, results are denoted J_u or δ_u and cannot be considered a geometry-independent material property.[7]

3 *J*-INTEGRAL AS A STRESS INTENSITY PARAMETER

The J-integral was proposed in 1968 by Rice[14] as a nonlinear energy release rate that could describe crack-tip conditions. Assuming the Ramberg-Osgood constitutive model and applying appropriate boundary conditions, Hutchinson[15] and Rice and Rosengren[16] proposed that stresses ahead of the crack tip could be estimated as

$$\sigma_{ij} = \sigma_{ys}\left(\frac{E \cdot J}{\alpha \cdot \sigma_{ys}^2 \cdot I_n \cdot r}\right)^{1/(n+1)} \cdot \tilde{\sigma}_{ij}(n,\theta) \quad , \tag{4}$$

where α is a dimensionless constant (usually unitary), I_n is an integration constant that depends on the hardening exponent n, $\tilde{\sigma}_{ij}$ is a dimensionless function and r and θ are the polar coordinates ahead of the crack tip in which stresses are desired. Equation (4) is known as the HRR singularity and the key aspect here is: as long as the stresses surrounding the crack tip are described by Eq. (4) (which means SSY condition), J uniquely characterizes crack-tip conditions for fracture and a critical value of J (J_c) is a size-independent measure of fracture toughness. This is the basis for the single-parameter EPFM.[1]

4 *J-Q* THEORY AND FAILURE LOCUS

Single-parameter elastic-plastic fracture mechanics breaks down in the presence of excessive plasticity, since the stress fields described by the HRR singularity are not more valid (stresses are “relaxed” as a result of local plastic deformation). The real stresses can alternatively be described in these cases as proposed by O’Dowd & Shih[17]: a combination of the HRR field and a difference field as

ISSN 1516-392X

$$\sigma_{ij} = (\sigma_{ij})_{HRR} + (\sigma_{ij})_{Diff.} \approx (\sigma_{ij})_{HRR} + Q \cdot \sigma_{ys} \cdot \delta_{ij} \ , \quad (5)$$

where δ_{ij} is the Kronecker Delta and Q is a parameter that quantifies the difference between real stresses and the reference field (HRR), in the form

$$Q = \lfloor \sigma_{yy} - (\sigma_{yy})_{HRR} \rfloor / \sigma_{ys} \ \ , \ at\ \theta = 0\ , \ for\ (r \cdot \sigma_{ys})/J = 2\ . \quad (6)$$

In a given cracked body, Q = 0 in the limit of SSY, but Q generally becomes increasingly negative with the evolution of deformation (increasing J). From a solid mechanics point of view, Q is a direct measure of stress triaxiality (constraint) at the crack tip. This variation of Q is highly sensitive to specimen thickness, loading mode and crack depth. Thin specimens, loaded under tension or containing shallow cracks favor excessive plasticity providing more negative Q values, as can be seen in a recent work of Flores et al.[18] Consequently, fracture toughness under low triaxiality conditions cannot be understood as a single value; rather, it is a function of Q and defines a failure locus, as presented by Fig. 3. The toughness locus is defined based on experiments which provide fracture toughness (e.g.: J_c values) for different Q values. Failure prediction for real structures can be conducted comparing the severity of the crack in the component (using local J-Q computations from finite element models as a crack driving force – see dashed line in Fig. 3) with the toughness locus.

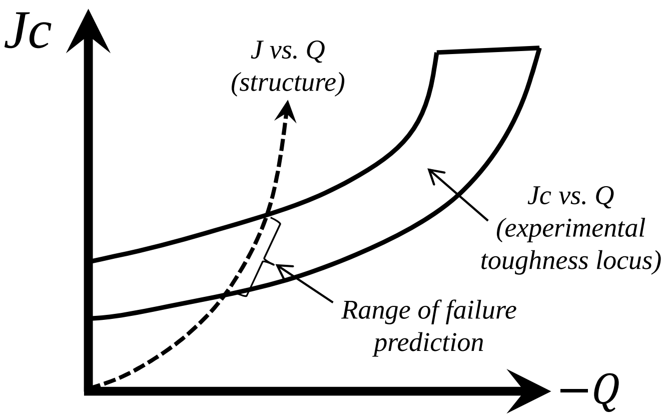

Figure 3. Schematic fracture toughness locus using J-Q theory. The evolution of J and Q in a cracked component is included to illustrate failure prediction using this methodology.[1]

5 EXPERIMENTAL PROCEDURES

5.1 Material Being Investigated

All specimens were made of a ferritic ASTM A516 Gr. 70 structural steel, obtained from hot rolled normalized plates (~ 20 mm thick). Previous studies conducted by the Donato[19] provided the conventional mechanical properties for this material (reproduced by Table 1).

ISSN 1516-392X

Table 1. Conventional mechanical properties (from tensile tests) of the material being investigated[19]

Material	E (GPa)	σ_{ys} (MPa)	σ_{uts} (MPa)	Area reduction (%)	H (MPa)	n
ASTM A516 Gr. 70	204.5	364	558	59.5	1010.5	4.22

In addition, the same document provides an estimate of the ductile-to-brittle transition temperature (DBTT) for this steel at -30ºC based on Charpy impact tests. However, due to the dynamic nature of Charpy impact tests, fracture mechanics testing at the same temperature tend not to characterize the material in the ductile-to-brittle transition region. As expected, some results from the same source indicated that J_c values could only be obtained for temperatures below ~ -70ºC. In this investigation, to test samples in the ductile to brittle region is of paramount relevance in order to be able to detect and describe triaxiality effects on fracture toughness and fracture micromechanisms.

5.2 Fracture Mechanics specimens, Apparatus and Testing Protocol

The SE(B) specimens follow ASTM E1820[7] statements, including thickness B = 18 mm, width $W = 2B$ = 36 mm and spam $S = 4W$ = 144 mm. All other geometric features follow Fig. 1. Considering valid results only, 21 shallow-cracked ($a/W \approx 0.20$) and 17 deep-cracked specimens ($a/W \approx 0.50$) could be prepared and tested. The samples were machined using CNC equipments for the external dimensions and Electrical Discharge Machining (EDM) for the notch. Fatigue precracking (comprising 1.5 - 2.0 mm crack extension) was conducted using the servohydraulic MTS 810 system presented by Fig. 4(a) according to the same standard and using sinusoidal loading with 15 Hz. Shallow-cracked samples demanded ~ 19 kN and deep-cracked ~ 8 kN.

Fracture tests were conducted using the same equipment and following ASTM E1820[7] in terms of loading rate and data post-processing (employing Eqs. 1-3). The desired low temperatures were achieved using absolute ethanol (> 99.8%) combined to dry ice. In this work, temperatures between -72ºC and -78ºC were employed and two thermocouples were used to guarantee deviations below ±1ºC during each test. Only the specimen was kept inside the cold bath (30 minutes for temperature stabilization plus testing time - see Fig. 4b), while the clip-gage was kept exposed to air (the temperatures achieved by the clip-gage did not violate its calibration temperature range). All post-mortem analysis were conducted based on image analysis as suggested by Barbosa and Donato.[20]

ISSN 1516-392X

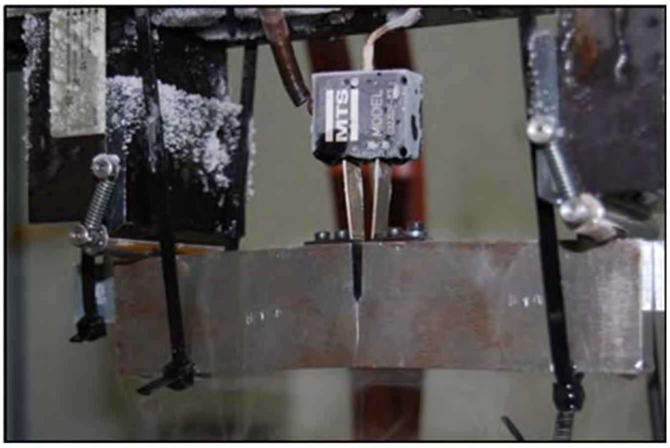

(a) (b)

Figure 4. (a) MTS 810 servohydraulic testing machine. (b) Bending apparatus and clip-gage for SE(B) specimens. Equipments available at the Metallic Materials Development Laboratory, FEI.

6 NUMERICAL PROCEDURES

6.1 Finite Element Models for SE(B) Specimens

Detailed finite element analyses were performed on 3-D models with the same geometrical features of the real SE(B) specimens. The analyses matrix included a/W = 0.2 and a/W = 0.5. Figure 5(a) illustrates the finite element models built for a/W = 0.5. It can be realized that the mesh pattern near the crack tip is highly refined and it derives from previous recommendations of Donato.[19] A conventional mesh configuration having a focused ring of elements surrounding the crack front is used with a small key-hole at the crack-tip; the radius of the key-hole, ρ_0, is 2.5μm (0.0025mm). Symmetry conditions permit modeling of only one-quarter of the specimen with appropriate constraints imposed on the remaining ligament (v = 0) and symmetry plane on half-thickness (w = 0). The quarter-symmetric model has 25 layers of elements to describe half-thickness and approximately 72000 8-node, 3-D tri-linear hexahedric elements (~ 77000 nodes). The finite element models are loaded by displacement increments imposed on the loading points to enhance numerical convergence.

In addition to the SE(B) geometries, a Modified Boundary Layer (MBL) model under plane strain condition was developed (see Fig. 5b) to define a reference stress field under SSY conditions to serve as a basis for Q calculation (see Eqs. 5-6). Details can be found in the work of Flores[21] and will not be provided here.

ISSN 1516-392X

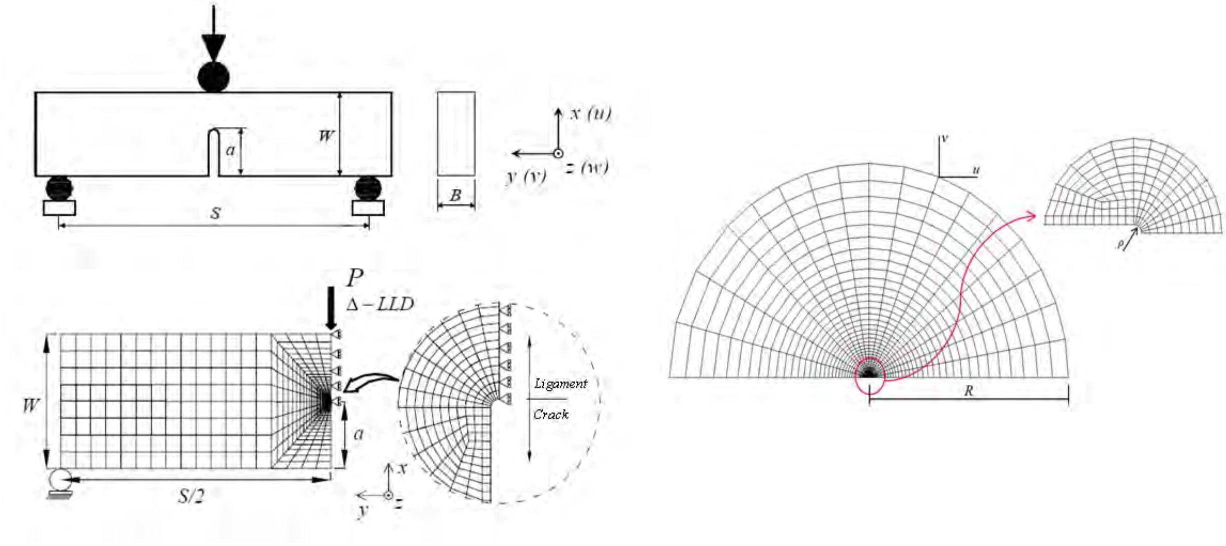

(a) (b)

Figure 5. (a) Loading strategy and mesh pattern (symmetric) for the developed SE(B) specimens. All models were 3D and considered thickness. (b) Modified Boundary Layer (MBL) model.

6.2 Numerical Solution

All models were processed using the research code WARP3D,[22] which incorporates a Mises (J_2) constitutive model in both small-strain and finite-strain framework. J-integral results derive from a domain integral procedure and presented strong path independence for domains defined outside the highly strained material near the crack tip. Q parameter was computed using JQCRACK software[23] for normalized radius $[r/(J.\sigma_{ys})] = 2$. The material constitutive model is elastic-plastic and was based on true stress-strain data obtained from tensile tests of the ASTM A516 Gr. 70 steel (elastic properties are E = 204.5 MPa and Poisson ratio ν = 0.3).

7 RESULTS

7.1 Fracture Toughness Results in Terms of J and CTOD

Figure 6(a,b) presents the obtained fracture toughness data (using Eqs. 1-3) as a function of relative crack depth respectively in terms of J-integral and $CTOD$ (δ). Solid markers represent critical data (with stable tearing inexistent or smaller than 0.2 mm – these data are denoted "c"). Open markers represent fracture toughness data which incorporate stable tearing (denoted "u").

First of all, the analysis of the abscissa shows that the precracking procedure provided original crack relative depths (a/W) very close to the desired values of 0.2 and 0.5. In addition, image analyses revealed that all precrack fronts were geometrically stable and were validated by ASTM E1820 requirements.[7]

In terms of fracture toughness results, conversely, it can be realized that a large scatter was obtained, specially considering shallow-cracked samples and non-critical ("u") data. In general, J and δ values for shallow cracks are higher than those for deep cracks. Further discussion here is necessary: considering post-mortem image analyses, 34% of the shallow-cracked samples presented stable tearing prior to unstable fracture (against 24% for deep cracked samples). In addition, the amount of stable tearing (in mm, see Fig. 2b) for shallow-cracked specimens was approximately 3 times greater than for deep-cracked ones, what was expected due to

ISSN 1516-392X

the lower stress triaxiality (constraint) of shallow-cracked specimens. This “extra” strain energy is computed by the eta method through the plastic area A_{pl} and can raise experimental fracture toughness as can be seen in Fig. 6. However, considering only critical (“c”) data, results between shallow and deep cracks are very close and a general trend of increase or decrease in toughness with crack depth is not clear.

As fracture phenomenon (cleavage) in the ductile-to-brittle transition region represents a material behavior that follows the weakest link theory[1], the description of toughness data using the Weibull statistics can be of great relevance to deal with the large scatter found, as presented next.

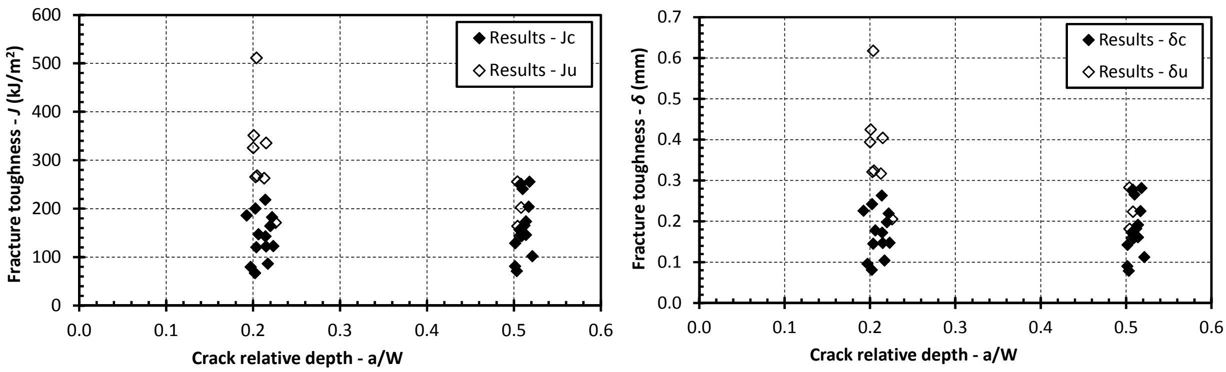

(a) (b)

Figure 6. Fracture toughness results for ASTM A516 Gr. 70 at ~ -75ºC considering (a) J-integral and (b) $CTOD$ (δ).

7.2. Fracture Toughness Description Using Weibull Statistics and Rffect of Crack Depth

Figure 7 presents, for J values, the same results of Figure 6 but represented using a bi-parametric Weibull distribution. Non-critical data were considered as censored values and details for this computations can be found in Anderson.[1]

First, it can be realized that both distributions are essentially linear and scatter is very reduced, which is necessary to provide a good description of fracture phenomenon by Weibull statistics. Second, the slopes of the distributions (which represent the Weibull moduli) are very close to the theoretical value of 2 for J[1] (they are respectively 2.2 for shallow cracks and 2.6 for deep cracks). It indicates that temperature was low enough to guarantee that cleavage controlled the fracture process and that the hypotheses of the weakest link theory were obeyed.

Figure 7(b) presents the characteristic fracture toughness results (J_0 – mathematically determined as the 63rd percentile of the distribution). The obtained results provided J_0 = 197 kJ/m^2 for deep cracks and J_0 = 213 kJ/m^2 for shallow cracks. It represents a slight increase of ~ 8% in fracture toughness as a result of shallow cracked SE(B) specimens and its lower stress triaxiality (constraint). This increase is much smaller than originally expected based on the literature. However, the good agreement of experimental data to the distributions of Fig. 7(a) indicates that this increase was experimentally observed.

ISSN 1516-392X

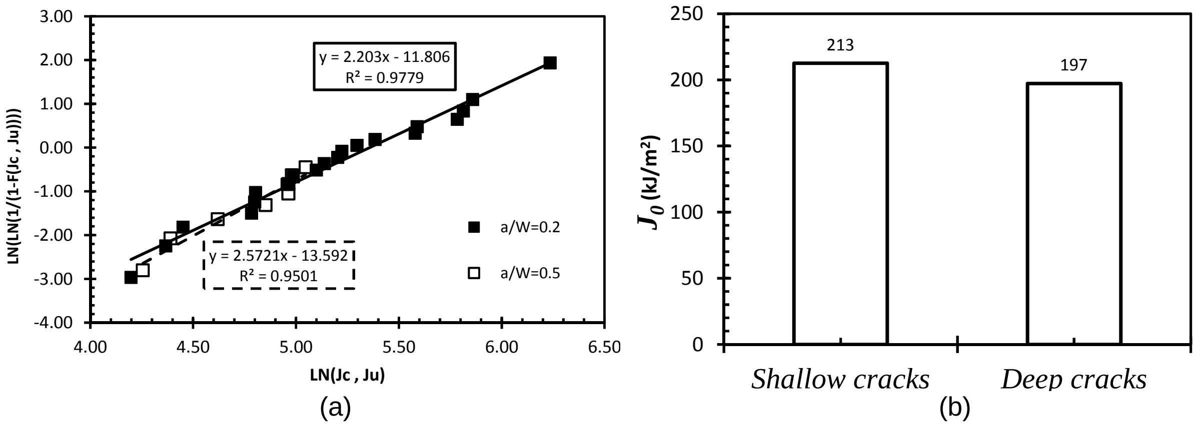

Figure 7. (a) Bi-parametric Weibull distribution of fracture toughness results for ASTM A516 Gr. 70 at ~ -75ºC. (b) Comparison of characteristic toughness values (J_0) for shallow and deep cracks.

7.3 *J-Q* Evolutions for the Studied Geometries

Figure 8 presents the *J-Q* evolutions obtained using the 3-D finite element models of both tested geometries. It can be realized both for shallow and deep cracks that: i) *Q* values are close to zero for low *J* values (*Q* = 0 means SSY condition, or the plain validity of HRR field and single-parameter fracture mechanics); ii) the greater is the applied *J* value, the more negative are respective *Q* values (it means larger loss of constraint or deviation from the reference SSY stress fields – see Eqs. 5-6). Consequently, results from Fig. 8 are in accordance with the literature and proves that shallow cracked SE(B) specimens (*a/W* = 0.2) present much larger loss of constraint (less stress triaxiality) if compared to deep cracked specimens (*a/W* = 0.5).

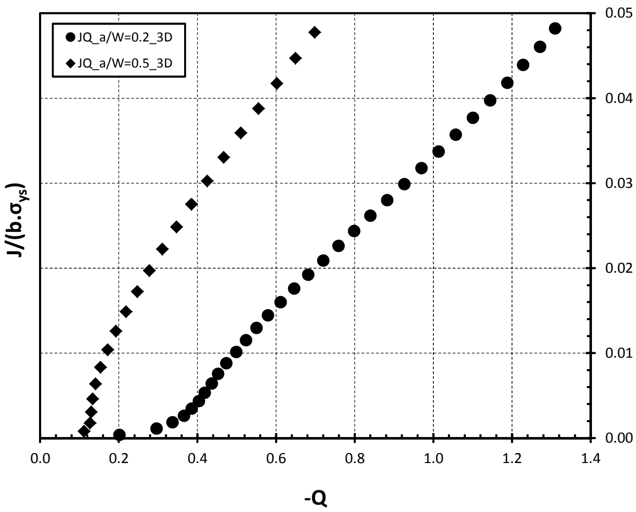

Figure 8. *J-Q* trajectories obtained from 3D finite element models for the tested SE(B) geometries.

Figure 9 combines the numerical *J-Q* trajectories presented by Fig. 8 with all fracture toughness results obtained in this investigation (see Fig. 6). Basically, each J_c or J_u value from Fig. 6 was plotted against the predicted *Q* value for that geometry and *J* level. Figure 9(a) represents *J* values in kJ/m^2 and is the basis for determining *J-Q* loci as illustrated by Fig. 3 (for real application, more geometries with different *Q* values should be tested). Figure 9(b) represents the same results but in terms of normalized dimensionless *J* values to make all results directly comparable.

ISSN 1516-392X

To enhance the comprehension of the results and the relevance of such J values for structural integrity evaluations, were included in Fig. 9 the maximum values of J (denoted here J_{max}) for the validity of SSY conditions and single-parameter fracture mechanics. These values are calculated as $J_{max} = (b.\sigma_{flow})/M$, where M is the so-called deformation limit(1) for each geometry and material. M values were calculated by the authors using plane strain finite element models of the SE(B) geometries of this work compared to a reference under SSY condition (aforementioned MBL models). Considering a 15% deviation on stresses normal to the crack plane and a normalized radius of $[r/(J.\sigma_{ys})] = 2$, were obtained $M \approx 27$ for deep-cracked SE(B) with $a/W = 0.5$ and $M \approx 161$ for $a/W = 0.2$.

The M values provided $J_{max} = 301.4$ kJ/m^2 for deep cracked specimens (which validates all results from $a/W = 0.5$ as capable of describing crack-tip stress fields in real structures – similitude principle – see Fig. 9a) and $J_{max} = 81.5$ kJ/m^2 for shallow cracked specimens (which validates only 10% of all obtained results from $a/W = 0.2$ – see Fig. 9a). Consequently, the combined results of Fig. 9 shows that more relevant than the small increase in the toughness values, the use of shallow-cracked SE(B) specimens creates a severe limitation regarding the validity of single-parameter fracture mechanics.

In practice, almost all values of fracture toughness obtained from SE(B) specimens with $a/W = 0.2$ cannot be directly employed for structural integrity evaluations as geometry-independent data. These results are geometry-dependent mechanical properties and demand finite element models both for the specimens and for the evaluated structures to match, for example, each J_c or J_u value with the respective Q value with which it was obtained (for example using the toughness locus approach of Fig. 3). This geometry-dependence of fracture toughness results usually demands a larger number of fracture tests and FE models to guarantee transferability between mechanical properties from small-scale laboratory samples and structures.

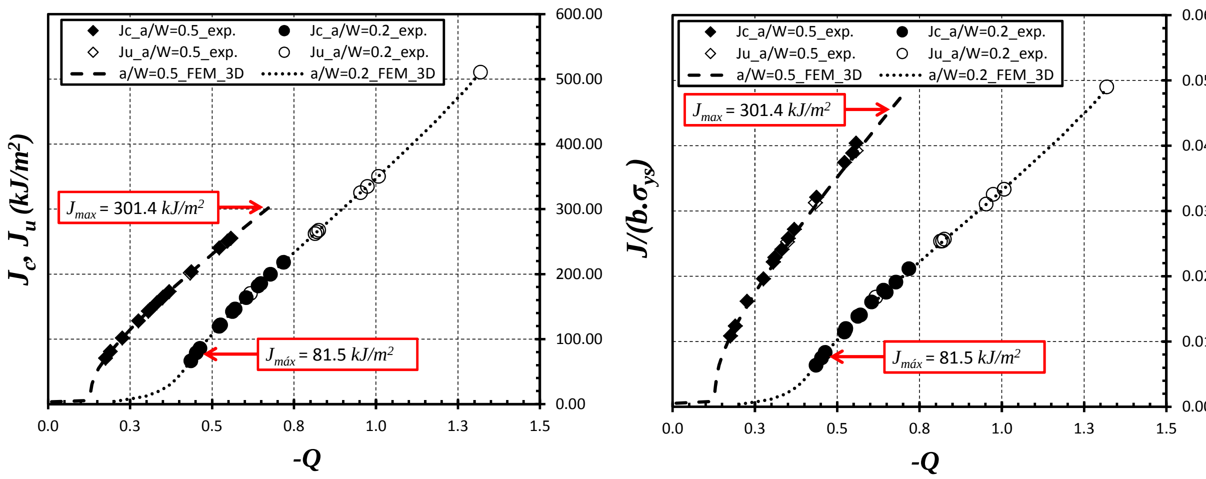

(a) (b)

Figure 9. J-Q trajectories obtained from 3D finite element models combined to fracture toughness results in terms of (a) J_c and J_u and (b) normalized J values.

8 CONCLUDING REMARKS

From this work, the following central conclusions emerge:

- The precracking strategy provided crack fronts validated by ASTM E1820 and with relative crack depths close to desired ratios ($a/W = 0.2$ and $a/W = 0.5$).

- Fracture toughness results in terms of J and δ presented large scatter, specially for shallow cracked specimens. However, all data could be very well described using bi-parametric Weibull distributions with slopes close to 2 for J. Consequently, testing temperatures can be considered to be in the ductile-to-brittle transition region.
- Q values demonstrated that shallow-cracked samples present much lower stress triaxiality. It is in accordance with the literature and experimental evidences of this work, since 34% of the shallow-cracked samples presented stable tearing prior to fracture, against 24% for the deep-cracked. In addition, tearing amount in shallow-cracked specimens was, in average, three times greater than for deep-cracked.
- The Weibull distributions (favored by the good agreement to experimental data – Fig. 7a) provided J_0 = 197 kJ/m^2 for deep cracks and J_0 = 213 kJ/m^2 for shallow cracks (a slight increase of ~ 8%). This increase is, however, much lower than originally expected based on the literature.
- Independent on the fracture toughness increase caused by different constraint presented by shallow cracked samples, the main effect of crack depth was on the significance of experimental J results as geometry-independent fracture toughness for the tested ASTM A516 Gr. 70 steel. While all results from samples with a/W = 0.5 were considered valid (respected SSY conditions) and geometry-independent mechanical properties that can be transferred to structures using single-parameter fracture mechanics, only 10% all obtained results from samples with a/W = 0.2 were valid. It means that fracture toughness data obtained from the tested shallow cracked specimens can only be employed supported by refined FE computations and J-Q toughness loci containing several experimental fracture results. In this case, this approach is only technically reasonable (and economically feasible) if the real structure being assessed present low stress triaxiality, cannot have its safety assured by geometry-independent fracture toughness from deep-cracked specimens, and demands large amounts of resources for maintenance or substitution.

Acknowledgment

This investigation was supported by FAPESP (Fundação de Amparo à Pesquisa do Estado de São Paulo) and by the Ignatian Educational Foundation (FEI, Brazil) through materials, laboratories and human resources.

REFERENCES

1 ANDERSON, T. L. **Fracture Mechanics: Fundamentals and Applications**, 3rd edition, New York, CRC Press, 2005, 640 p.
2 AMERICAN PETROLEUM INSTITUTE. **API RP 579-1: Recommended Practice for Fitness-for-Service**, 2nd edition, 2007, 1126 p.
3 BRITISH STANDARDS INSTITUTION. **BS 7910:2005: Guide to methods for assessing the acceptability of flaws in metallic structures**, England, 2005, 306 p.
4 HARRISON, R.P.; LOOSEMORE, K.; MILNE, I.; DOWLING, A.R. **Assessment of the Integrity of Structures Containing Defects**, CEGB Report R/H/R6 – rev. 2, Central Electricity Generating Board, United Kingdom, 1980.
5 STRUCTURAL INTEGRITY ASSESSMENT PROCEDURES FOR EUROPEAN INDUSTRY. SINTAP; Final Report, July, 1999.
6 DET NORSKE VERITAS. **DNV-OS-F101: Submarine Pipeline Sys.**, Norway, 2012.
7 AMERICAN SOCIETY FOR TESTING AND MATERIALS. **ASTM E 1820: Standard Test Method for Measurement of Fracture Toughness**, Philadelphia, 2011.

ISSN 1516-392X

8 AMERICAN SOCIETY FOR TESTING AND MATERIALS. **ASTM E 1290: Standard Test Method for CTOD Fracture Toughness Measurement**, Philadelphia, 2008.
9 INTERNATIONAL ORGANIZATION FOR STANDARDIZATION. **ISO 12135: Metallic materials - Unified method of test for the determination of quasistatic fracture toughness**, Switzerland, 2002.
10 MOREIRA, F. C., DONATO, G. H. B. **Estimation Procedures for J and CTOD Fracture Parameters Experimental Evaluation using Homogeneous and Mismatched Clamped SE(T) Specimens**, Pressure Vessel and Piping, 2010.
11 CRAVERO, S., RUGGIERI, C. **Correlation of Fracture Behavior in High Pressure Pipelines with Axial Flaws Using Constraint Designed Test Specimens - Part I: Plane-Strain Analyses**, Engineering Fracture Mechanics, Vol.72, 2005, p. 1344-1360.
12 CRAVERO, S., RUGGIERI, C. **A two-parameter framework to describe effects of contraint loss on cleavage fracture and implications for failure assessments of cracked components**. Journal of the Brazilian Society of Mechanical Sciences and Engineering. V.25, n.4, 2003.
13 DONATO, G. H. B., MAGNABOSCO, R., RUGGIERI, C. **Effects of Weld Strength Mismatch on J and CTOD Estimation Procedure for SE(B) Specimens,** International Journal of Fracture, Vol.159, 2009, p. 1-20.
14 RICE, J. R. **A Path Independent Integral and the Approximate Analysis of Strain Concentration by Notches and Cracks**. Journal of Applied Mechanics, V. 35, 1968, p. 379-386.
15 HUTCHINSON, J. W. **Singular Behavior at the End of a Tensile Crack Tip in a Hardening Material**. Journal of the Mechanics and Physics of Solids, V. 16, 1968, p. 13-31.
16 RICE, J. R., ROSENGREN, G. F. **Plane Strain Deformation Near a Crack Tip in a Power-Law Hardening Material**. Journal of Applied Mechanics, V. 16, 1968, p. 1-12.
17 O'DOWD, N. P., SHIH, C. F. **Family of Crack-Tip Fields Characterized by a Triaxiality Parameter – I. Structure of Fields**. Journal of the Mechanics and Physics of Solids, V. 39, 1991, p. 898-1015.
18 FLORES, W. D., DOS SANTOS, O. J., GODEFROID, L. B, DONATO, G. H. B. **Avaliação da Geometria do Corpo de Prova na Tenacidade à Fratura de Aço API-5L-X70**. 67th International ABM Congress, 2012.
19 DONATO, G. H. B. **Efeitos de Heterogeneidade Mecânicas sobre Forças Motrizes de Trinca em Juntas Soldadas: Determinação Experimental de Tenacidade e Extensão de Metodologias de Avaliação de Criticidade de Defeitos**. PhD. thesis, Polytechnic School of the University of São Paulo, 2008.
20 BARBOSA, A. C., DONATO, G. H. B. **Desenvolvimento e Validação Experimental de Algoritmo para Medição de Pré-trinca de Fadiga e Crescimento Estável Utilizando Análise Digital de Imagens**.66th International ABM Congress, 2012.
21 FLORES, W. D. **Avaliação da Geometria do Corpo de Prova na Tenacidade à Fratura de Aço API-5L-X70**. Master thesis, Universidade Federal de Ouro Preto (UFOP), 2012.
22 KOPPENHOEFER, K.; GULLERUD, A.; RUGGIERI, C.; DODDS, R.; HEALY, B. **WARP3D: Dynamic Nonlinear Analysis of Solids Using a Preconditioned Conjugate Gradient Software Architecture**, Structural Research Series (SRS) 596. UILU-ENG-94-2017. University of Illinois at Urbana-Champaign, 1994.
23 CRAVERO, S., RUGGIERI, C. **JQCRACK V1.0 - Cálculo numérico do parâmetro hidrostático Q para componentes estruturais 2D contendo trinca**. Technical Report of the Polytechnic School of the University of São Paulo – BT/PNV/59, 2002.